HHS Public Access

Author manuscript

Sci Immunol. Author manuscript; available in PMC 2022 June 10.

Published in final edited form as:

Sci Immunol. 2021 December 10; 6(66): eabj0789. doi:10.1126/sciimmunol.abj0789.

Infant T cells are developmentally adapted for robust lung immune responses through enhanced T cell receptor signaling

Puspa Thapa[1], **Rebecca S. Guyer**[1], **Alexander Y. Yang**[1], **Christopher A. Parks**[2,3], **Todd M. Brusko**[4], **Maigan Brusko**[4], **Thomas J. Connors**[5], **Donna L. Farber**[1,6,*]

[1]Department of Microbiology and Immunology, Columbia University Irving Medical Center, New York NY 10032

[2]Columbia Center for Translational Immunology, Columbia University Irving Medical Center, New York, NY 10032

[3]Department of Medicine, Columbia University Irving Medical Center, New York, NY 10032

[4]Department of Pathology, Immunology and Laboratory Medicine, University of Florida, Gainesville, FL 32611

[5]Department of Pediatrics, Columbia University Irving Medical Center, New York, NY 10032

[6]Department of Surgery, Columbia University Irving Medical Center, New York, NY 10032

Abstract

Infants require coordinated immune responses to prevent succumbing to multiple infectious challenges during early life, particularly in the respiratory tract. The mechanisms by which infant T cells are functionally adapted for these responses are not well understood. Here, we demonstrated using an *in vivo* mouse co-transfer model that infant T cells generated greater numbers of lung-homing effector cells in response to influenza infection compared to adult T cells in the same host, due to augmented T cell receptor (TCR)-mediated signaling. Mouse infant T cells showed increased sensitivity to low antigen doses, originating at the interface between T cells and antigen-bearing accessory cells--through actin-mediated mobilization of signaling molecules to the immune synapse. This enhanced signaling was also observed in human infant versus adult T cells. Our findings provide a mechanism for how infants control pathogen load and dissemination, which is important for designing developmentally-targeted strategies for promoting immune responses at this vulnerable life stage.

One Sentence Summary:

*Correspondence: df2396@cumc.columbia.edu.

Author contributions

P.T. designed and performed experiments, analyzed data, and wrote the manuscript; R.S.G. and A.Y. performed experiments and analyzed data. C.A.P. designed experiments and analyzed data. T.B. and M.B. coordinated acquisition of human infant tissues. T.C. coordinated acquisition and processing of human infant tissue. D.L.F planned experiments, analyzed data, wrote and edited the manuscript.

Competing Interests: Authors declare that they have no competing interests.

Data and material availability:

All data are available in the main text or the supplementary materials.

Enhanced T cell activation and immune synapse formation by infant T cells promotes generation of lung homing effector cells.

Keywords

Lung immunity; respiratory infection; Effector differentiation; Infant immunity

INTRODUCTION

During early life, infants encounter multiple diverse pathogens, including pathogens that infect the respiratory tract against which they are particularly vulnerable. Infants are more susceptible to morbidity and mortality to ubiquitous respiratory viruses such as influenza and respiratory syncytial virus (RSV) and experience recurrent respiratory tract infections due to lack of long-term protective immunity that is well-established in adults (1, 2). However, infants can mount effective responses to these and other respiratory viruses, including SARS-CoV-2 during the current pandemic (3, 4), suggesting that the early life immune system may have specific mechanisms in place for efficacious anti-pathogen immunity. Moreover, infants and young children exhibit distinct responses to vaccines compared to adults, although vaccine formulations are the same for all ages (5, 6). Understanding the mechanisms for the distinct immune responses to respiratory viruses in early life and childhood is important for protecting infants from current and emerging pathogens.

The reduced ability of infants to combat viral respiratory infections is attributed to the immaturity of adaptive immunity mediated by newly developed naïve T cells (7, 8). However, recent studies show that infant immune responses to infection are not necessarily of lower magnitude compared to adults, but rather exhibit distinct functional features and altered T cell differentiation fates (9, 10). In response to systemic and respiratory virus infection, infant $CD8^+$ and $CD4^+$ T cells exhibit enhanced proliferation and/or differentiation to effector cells, and reduced memory formation (11-13) . These distinct responses of neonatal T cells in part derive from their maturation from fetal progenitors compared to T cells generated during the post-natal period, resulting in altered transcriptional profiles (12, 14). The induction and expression levels of the transcription factor T-bet can bias effector over memory T cell fate in adult mouse T cells, and we previously showed that reducing T-bet expression in infant T cells reduces effector generation *in vivo* (11, 15). Another transcription factor determining T cell fate, T cell factor-1 (TCF-1), is required for memory formation and inhibits effector formation (16-18), though its role in infant T cell differentiation is not known. Moreover, the upstream mechanisms driving differential activation and fate determination in infant T cells remains unclear.

Antigen-mediated activation of T cells triggers T cell-receptor (TCR)-coupled signaling events which lead to transcription factor activation. T cell activation begins with the formation of an immune synapse (IS) between the T cell and antigen presenting cell (APC) which contain the molecular contact points between the TCR, major histocompatibility

complex (MHC) complexed with antigen, the CD4 or CD8 co-receptor, and integrins such as LFA-1 (CD11a) (19-21). IS formation and maintenance is essential for initiation and propagation of proximal signaling events including phosphorylation of CD3 chains by the co-receptor–coupled p56Lck tyrosine kinase, thereby governing the magnitude of TCR-mediated signaling (22, 23). TCR signal strength also influences differentiation with stronger TCR signal strength biasing effector differentiation over memory T cell fate (24-26). Differential TCR-mediated signaling in thymocytes versus peripheral T cells and naïve versus memory T cells is described; however, it is not known whether T cell activation and TCR-coupled signaling are developmentally regulated in T cells in early life.

In this study, we investigated the molecular mechanisms for the distinct responses of infant compared to adult T cells in mice and humans. Using a co-transfer mouse model to track the intrinsic activation properties of infant and adult mouse T cells in response to respiratory infection in the same host, we found that virus-specific infant T cells exhibited increased proliferation and generation of lung-homing effector T cells compared to adult T cells in the same host. These distinct mouse infant T cell responses involved extensive downregulation of TCF-1, along with increased proximal signaling events upstream of TCF-1. We mapped the initiating events in enhanced infant T cell responses to IS formation in response to antigenic stimulation. We further confirmed that human infant T cells exhibited enhanced TCR sensitivity, signaling, as well as augmented TCF-1 downregulation relative to adult T cells. Our findings demonstrate that infant T cells are uniquely adapted for robust responses to combat antigenic challenges during early life, with implications for the design of age-targeted strategies for boosting immunity in this critical life stage.

RESULTS

Enhanced generation of lung-homing effector cells by infant compared to adult T cells during respiratory virus infection

To study intrinsic properties of infant versus adult T cells to influenza infection, we established a co-transfer mouse model to follow the fate of infant or adult-derived influenza-specific $CD4^+$ T cells *in vivo* in multiple tissue sites within the same host. Infant T cells were obtained from mice 10-14 days old, the timepoint where mouse neonatal T cells are most similar in phenotype to human infant T cells (11). Adult T cells were obtained from mice over 6 weeks of age. We transferred equal numbers of $CD4^+$ T cells from infant and adult OT-II TCR transgenic mice, expressing a transgene-encoded TCR specific for chicken ovalbumin (27), into congenic adult mouse hosts. Prior to transfer, there were similar frequencies of OT-II cells in adult and infant mice and comparable expression levels of the OT-II TCR (Vα2/Vβ5.1) (figure S1A). Both infant and adult OT-II cells exhibited a predominant naïve ($CD62L^{hi}CD44^{lo}$) phenotype (figure S1B). Host mice were subsequently challenged with recombinant influenza virus expressing the OT-II-specific epitope (PR8-OVA, Fig. 1A). Differential expression of congenic markers was used to distinguish between transferred infant, adult, and host T cells in the lung and lung-draining mediastinal lymph node (medLN) at indicated times post-infection. Prior to infection, the frequencies of infant and adult OT-II cells in host LN were equivalent (Fig. 1B), indicating comparable persistence after transfer.

T cell responses to influenza virus are typically primed in the medLN where they develop into lung-homing effector cells which direct lung viral clearance *in situ* (28, 29). At early times post-infection, (day 4 p.i.) there was a significantly higher proportion of infant compared to adult T cells in the medLN (Fig. 1C, figure S1C), which also exhibited increased proliferation compared to adult T cells (Fig. 1C, D, figure S1E). Few undivided OT-II cells (infant or adult origin) had migrated to the lungs at this early time point (figure. S1D). During the peak T cell response (day 7-15 p.i.) infant T cells outnumbered adult T cells in the lungs by 4:1 in frequency and absolute number but were present in comparable frequency and numbers to adult T cells in the mediastinal lymph nodes (Fig. 1E-G). Furthermore, the ratio of OT-II cells in the lung relative to medLN was higher for infant T cells compared to adult T cells within each congenic host (Fig. 1H). Infant and adult lung effector T cells exhibited comparable Annexin V staining (with modest increase in infant T cells) (figure S1F), indicating that their different numbers in the lung were not due to variations in cell death. Functionally, infant and adult lung OT-II effector cells secreted proinflammatory cytokines IFNγ and TNFα and low-to-negligible levels of IL-4, IL-5, and IL-17A (figure S1G); however, there were significantly higher frequencies of infant OT-II cells producing both IFNγ and TNFα in the lung compared to adult cells (Fig. 1I). These findings show that infant T cells have an enhanced capacity compared to adult T cells to proliferate and differentiate into lung-homing effector cells in response to respiratory virus infection.

Infant T cells downregulate TCF-1 for enhanced proliferation

We investigated whether the enhanced proliferation and differentiation of infant T cells was due to differential regulation of key transcription factors TCF-1 and T-bet, required for self-renewal and proinflammatory effector function, respectively (18, 30, 31). TCF-1 is highly expressed in naïve T cells, becomes downregulated during effector differentiation, and retention of TCF-1 expression is required for memory T cell development and persistence (16, 32). Prior to infection, infant OT-II cells expressed slightly higher levels of TCF-1 compared to adult OT-II cells (figure S2A). At day 4 p.i. in the medLN, proliferating infant T cells (detecting by dilution of the proliferation dye CPD) downregulated TCF-1 to a greater extent than proliferating adult T cells, while non-dividing (CPD^{hi}) infant T cells maintained slightly higher TCF-1 expression compared to adult T cells (Fig. 2A, figure S2B). In the lung (day 7-15 p.i), only a small fraction of infant OT-II cells maintained TCF-1 expression compared to a higher proportion of adult OT-II cells expressing TCF-1 (Fig. 2B). At the same timepoints, T-bet expression was elevated in both infant and adult lung OT-II cells, compared to the lower level expressed in host naïve T cells (figure S2C), indicating their differentiation to effector cells. Together, these finding show enhanced expansion of lung homing infant effector T cells is accompanied by an early and more rapid downregulation of TCF-1 compared to adult effector $CD4^+$ T cells.

To determine whether TCF-1 played a direct role in the enhanced proliferation of infant T cells, we generated OT-II mice with fixed expression of TCF-1 (OT-II/TCF-1 Tg) by crossing to TCF-1 transgenic mice (see Mice *section* in Materials and Methods (33)). Equal numbers of infant OT-II/TCF-1 Tg and adult OT-II T cells were co-transferred into congenic hosts and subsequently challenged with PR8-OVA as in Fig. 1A. Prior to viral

challenge, Infant OT-II/TCF-1 Tg T cells expressed higher levels of TCF-1 (which exhibited a bimodal expression pattern) compared to adult WT OT-II as measured in the medLN (Fig. 2C). Following PR8-OVA challenge, the frequency and number of infant OT-II/TCF-1 Tg was similar to adult OT-II T cells in the lungs, but was reduced compared to adult OT-II cells in the medLN (Fig. 2D, E; figure S2D). As a result, the ratio of OT-II cells in the lung compared to medLN in congenic hosts was higher for infant TCF-Tg compared to adult OT-II cells (Fig. 2F), similar to our findings with OT-II (non-TCF-Tg) infant T cells (Fig. 1H). These findings show that fixing TCF-1 expression in infant T cells constrained proliferative expansion; however, the biased differentiation to lung homing effector cells by infant T cells was upstream of TCF-1 expression.

Enhanced TCR-mediated signaling by infant T cells *in vivo*

We hypothesized that the enhanced effector differentiation by infant T cells could be driven by the more proximal events involved in T cell activation and signaling. To measure the extent of TCR-mediated signaling to influenza infection *in vivo* in the co-transfer model, we assessed the expression levels of the OT-II TCR as programmed downregulation of the TCR correlates with TCR signal strength (34). When measured using a specific tetramer that binds to the OT-II TCR (35), both infant and adult OT-II cells in LNs had comparable tetramer binding prior to influenza challenge (Fig. 3A), consistent with comparable surface expression of the Vα2Vβ5.2 TCR (figure S1A). Following influenza challenge, however, the pattern of tetramer binding is reduced relative to uninfected for both infant and adult OT-II cells that was observed at day 11 and 15 post-infection (Fig. 3A, figure S3A). Importantly, infant lung OT-II and had significantly reduced tetramer binding compared to adult OT-II cells in the lungs (Fig. 3A. figure S3A); a similar reduction in tetramer binding was also observed between infant TCF-1 Tg OT-II cells and adult OT-II cells in the lung (Fig. 3B; figure S3B). These results suggest that TCR downregulation is upstream of TCF-1 expression, which is further supported by similar tetramer binding between $TCF1^{high}$ and $TCF1^{low}$ effector OT-II cells in both infant and adults (figure S3C). Together, these results suggest enhanced TCR-coupled proximal signaling by infant compared to adult T cells.

Augmented TCR sensitivity by infant T cells lowers the activation threshold

We further investigated whether enhanced TCR downregulation as observed *in vivo* by infant T cells was indicative of increased sensitivity of infant T cells to antigenic stimulation. We therefore stimulated infant and adult OT-II T cells with varying doses of OVA peptide antigen in the presence of adult-derived antigen-presenting cells (A-APC) and assessed multiple readouts for TCR-mediated activation and signaling at different time points. Infant OT-II cells exhibited increased and more rapid proliferative responses to lower peptide doses (0.01-0.1μg) compared to adult OT-II cells (Fig. 4A, figure S3D). Infant T cells also expressed higher levels of the activation markers CD69 and CD25 at lower peptide doses compared to adult T cells (Fig. 4B). Moreover, there was significantly higher induction of the transcription factor Nur77, an orphan nuclear receptor which is a marker of early TCR-mediated signaling (36-38) and IRF4, which is directly downstream of TCR signaling (39, 40) by infant compared to adult T cells at low and intermediate antigen doses (Fig. 4C). To determine whether the enhanced activation of infant T cells was due to A-APC, we set up similar stimulations with infant-derived APC (I-APC). Accordingly, infant OT-II

cells exhibited enhanced proliferation, activation, and signaling compared to adult OT-II cells when stimulated in the presence of OVA+ I-APC (Fig. 4D). These results demonstrate a dramatically higher antigen sensitivity and reduced activation threshold for infant T cells compared to adult T cells, independent of the mode of stimulation. These findings suggest that infant T cells are more readily activated in conditions of limited antigen availability.

Increased TCR-coupled signaling by infant compared to adult T cells is developmentally regulated

Manifestations of TCR-coupled signaling occur within minutes to hours following antigen-mediated stimulation. We therefore assessed early timepoints for TCR downregulation and Nur77 upregulation in antigen-stimulated infant and adult OT-II cells. Infant OT-II cells exhibited more rapid kinetics of surface TCR-β downmodulation compared to adult OT-II cells, starting at 2hrs post- antigen stimulation which was reduced further up to 8hrs post-stimulation (Fig. 5A). Infant T cells also showed a more rapid and enhanced upregulation of Nur77 expression at early timepoints relative to adult T cells (Fig. 5B), that was also observed in the presence of I-APC (figure S4). These results indicate that the enhanced activation of infant T cells occurs at early kinetics.

We then asked whether this enhanced signaling by infant compared to adult T cells was developmentally regulated during early life, by obtaining OT-II T cells at different post-natal ages for analysis of antigen-driven activation. Nur77 upregulation was enhanced in OT-II cells obtained from by mice at postnatal day (PND) 14, 21 and 28 compared to adult OT-II cells (Fig. 5C). However, the signaling enhancements over adult T cells observed in younger T cells (measured by fold-change PND/adult mice) were higher in PND 14 mice relative to PND 21 and 28 mice; T cells from PND 28 mice were closest to adult T cells in the extent of signaling (Fig. 5C). These results suggest that enhanced TCR sensitivity and signaling is highest in T cells during the initial weeks of life and adopts a more measured response during maturation over the first month of life.

We also assessed early signaling events proximal to Nur77 such as phosphorylation of ERK1/2, a proximal signaling event that occurs following activation of TCR-coupled tyrosine kinases (41). An increased proportion of infant $CD4^+$ T cells phosphorylated ERK1/2 at earlier times following TCR engagement, compared to adult $CD4^+$ T cells, while there was no significant difference in pERK1/2 expression upon phorbol 12-myristate 13-acetate (PMA)/ionomycin stimulation which bypasses the TCR (Fig. 5D, E). These results indicate that infant $CD4^+$ T cells have an intrinsic capacity for enhanced proximal TCR-coupled signaling compared to adult T cells responding to the same antigenic epitope.

Infant T cells more readily form immunological synapses with antigen-bearing accessory cells

TCR activation and early signaling are triggered when the TCR and accessory molecules, bind their respective ligands on the surface of an antigen presenting cell (APC) forming an immunological synapse (IS) at the point of contact (19, 42). Key molecules in the mature IS include LFA-1(CD11a), an integrin for stable conjugate formation, actin, for overall mobilization of signaling molecules to the TCR, and p56lck kinase, an essential tyrosine

kinase coupled to the CD4 and CD8 co-receptors (43-45). To determine if the distinct TCR signaling capacity of infant compared to adult T cells is regulated at the level of IS formation, we employed imaging flow cytometry to visualize T cells in contact with APC (46, 47) and key molecules associated with IS formation in the presence or absence of the antigenic stimulus (see methods). OT-II cells and APCs were distinguished by differential fluorescent labeling as well as expression of surface and intracellular markers expressed by each cell and in the contact zone between them (Fig. 6A).

Unstimulated infant and adult T cells expressed comparable levels of CD3, CD4, intracellular Lck, and LFA-1 (figure S5A) and did not form IS when present in conjugates with APC in the absence of antigen, as manifested by the broad distribution of CD3 and actin around the cell perimeter (Fig. 6B). Upon stimulation with cognate antigen, there was a shift in distribution of CD3, LFA-1, actin, p56lck, and CD4 to the zone of contact between the T cell and the APC within 10 minutes and maintained through 60 minutes indicating stable IS formation for both infant and adult cells (figure. S5B, Fig. 6B-D). However, there were significantly higher levels of actin, p56lck, and CD4 in the IS of infant compared to adult OT-II cells at all timepoints (Fig. 6E-G), while accumulation of LFA-1 within the IS was similar between infant and adult T cells (figure. S5B). Furthermore, there was enhanced co-localization of CD4/p56lck with CD3, and CD4 with CD3 in infant compared to adult T cells at all timepoints, while co-localization of CD11a with CD3 was only significant at 10min (figure S5C, D). Infant OT-II cells also showed significantly increased accumulation of actin in the IS compared to adult OT-II cells even when stimulated at a low peptide dose (figure S5E). Together, these findings indicate that increased TCR-coupled signaling by infant compared to adult T cells originates at the earliest stage in T cell activation— through actin-mediated mobilization of signaling molecules to the IS.

Human infant T cells exhibit enhanced TCR-coupled signaling and TCF-1 downregulation

To address if human infant T cells exhibit similar enhancements in TCR-coupled signaling and differentiation compared to adult T cells, we examined the response of purified naïve $CD4^+$ T cells isolated from infant and adult lymph node T cells to polyclonal activation by anti-CD3/anti-CD28/anti-CD2-coupled beads, as surrogates for an antigen-driven response. Human infant T cells showed higher levels of Nur77 expression at early timepoints compared to adult T cells (Fig. 7A, figure S6A). Human infant T cells also exhibited reduced TCF-1 expression upon proliferation and a higher proliferative index compared to adult T cells (Fig. 7B,C). Importantly, infant T cells had a reduced capacity to retain TCF-1 expression following activation compared to adult cells, as exemplified by lower TCF-1 levels early in proliferation, starting at division 3 (Fig. 7D, E). Production of TNF-α and IFN-γ was similar between infant and adult naïve $CD4^+$ T cells after 4 days of stimulation (figure S6B), indicating that human infant T cells can mediate robust effector responses, consistent with findings in mice that infant T cells migrating to the lungs during infection showed robust effector function (Fig. 1F). These results indicate that human naïve T cells also show age-dependent capacities for TCR-mediated activation; those derived early in life have an enhanced capacity for TCR-coupled signaling driving effector differentiation compared to naïve T cells which persist in adults.

DISCUSSION

Infancy is a unique period of exposure and immune education to multiple new pathogens, particularly for those encountered in the respiratory tract. While the naiveté of adaptive immunity during infancy has been attributed to an overall weaker immune system, the emerging view from a number of studies indicate that infant T cells exhibit altered functional responses compared to adult T cells (8, 11, 12, 14). However, the basic mechanisms for these distinct responses remain incompletely understood. In this study, we demonstrated that infant T cells were intrinsically adapted to mediate augmented responses to influenza infection *in vivo* and low dose antigenic stimulation *ex vivo* due to increased TCR-coupled signaling originating at the most proximal stage of T cell activation—IS formation. This enhanced TCR-coupled signaling resulted in an intrinsic bias for differentiation to tissue-homing effector cells that governs early responses to respiratory pathogens, and was recapitulated in human infant T cells. Our findings may help to inform strategies for promoting immunity at early life stages.

We used a co-transfer model of infant and adult TCR transgenic OT-II T cells recognizing a single antigenic epitope within a recombinant influenza strain to compare antigen-specific responses to infection that were intrinsic to infant or adult T cells. Importantly, infant virus-reactive T cells exhibited robust proliferation in response to influenza infection, out-pacing expansion of adult-derived T cells and outcompeting them in the lung. This expansion was accompanied by downmodulation of the transcription factor TCF-1 to a greater extent in infant than adult T cells, consistent with the known reduction in TCF-1 expression during proliferative expansion and effector differentiation (16, 18). T cells from infant TCF-Tg mice with fixed expression of TCF-1 exhibited comparable proliferation as adult WT T cells; however, , TCF-1-Ttg infant T cells still exhibited biased lung homing compared to adult T cells. These findings indicated that signals upstream of TCF-1 activity were regulating distinct responses in infants. These upstream TCF-1-independent processes in infant T cells occurred at the level of TCR-mediated signal transduction.

We found enhanced TCR-mediated proximal signaling in infant compared to adult T cells, as manifested by TCR downregulation, Erk phosphorylation and induction of Nur77. Moreover, these distinct responses of infant T cells originated at the earliest stage of T cell activation during IS formation. The initial discovery of the IS provided evidence for structural organization of the T cell-APC conjugate as a critical requirement for TCR-coupled signaling and subsequent activation outcomes (21, 42, 43). Infant T cells generate mature IS with increased kinetics compared to adult T cells and mobilize greater quantities of actin, CD4 and Lck to the IS, despite expressing comparable levels of these molecules as adult cells. The co-expression of Lck with CD4 was not different between infant and adult T cells at all timepoints, suggesting, there may be other factors that influence Lck/CD4 mediated TCR signaling in infant T cells (22, 48-51). As the cytoskeleton and membrane dynamics can affect IS formation (21, 52), differences in membrane fluidity or structure of infant T cells may facilitate their interaction with APC. Further investigation of the biophysical properties of infant relative to adult T cells may provide additional insight into this process.

We showed enhanced TCR sensitivity of infant T cells compared to adult T cells using antigenic stimulation of OT-II TCR transgenic $CD4^+$ T cells, by polyclonal stimulation of $CD4^+$T cells from wildtype mice, and polyclonal stimulation of T cells from human infant lymph nodes. These findings are consistent with results showing robust expansion of infant $CD4^+$T cells expressing a different transgenic TCR specific for an influenza epitope (53), and increased proliferative responses of infant compared to adult $CD8^+$T cells expressing a transgenic TCR specific for Listeria (12). These findings suggest that enhanced immune synapse formation and TCR signaling by infant T cells is an intrinsic features of early life T cells that is independent of antigen specificity. Determining how individual TCRs of different avidities may impact IS formation during early life is a crucial future step.

The specific responses of infant T cells may derive from their origin and/or recent emergence from the thymus. Neonatal T cells present at birth are derived from fetal bone marrow progenitors and these T cells have distinct transcriptional profiles compared to T cells generated postnatally (14). For our studies, we obtained T cells at later stages of infancy in mice, allowing for 10- 14 days of post-natal development and we show similar enhanced signaling in human T cells up to 2 years of age. Mouse models examining recent thymic emigrants (RTE) marked by green fluorescent protein (GFP) expression also identified enhanced proliferation and responses by RTE compared to naïve T cells which persisted in the periphery (54). While these results suggest that some of the findings may be due to newly developed naïve T cells, RTE were also found to be impaired in effector and proinflammatory cytokine production (54, 55), unlike other studies with neonatal T cells (56, 57) and infant T cells examined here. Together, our findings suggest that developmental origin and “newness” may contribute to the distinct activation properties of infant T cells, in addition to other factors.

The higher TCR-coupled signaling strength of infant T cells results in increased sensitivity to low antigen doses compared to adult T cells. The ability of infants to generate adaptive immune responses to minute levels of antigen, could facilitate protection from viruses which replicate exponentially in the host. Enhanced TCR signaling could also explain the advantage of infants and young children in generating efficacious primary responses to novel pathogens, like SARS-CoV-2 which rarely infects infants and exhibits reduced infection and dissemination in children compared to adults (3, 4, 58). Higher sensitivity T cell responses can promote clearance of low viral doses, preventing viral replication and dissemination to pathogenic levels as seen in adults (59). Whether this enhanced sensitivity of infant T cells in humans is maintained throughout childhood remains to be determined, though recent evidence shows distinct immune responses for children of all ages compared to adults to respiratory challenge (58). Future studies defining both anti-viral and vaccine responses in children of different ages can enable age-targeted strategies for immune modulation at this formative life stage.

MATERIALS AND METHODS

Study design:

The aim of the study was to investigate the molecular mechanisms that govern infant $CD4^+$ T cell responses to influenza infection. We used a murine influenza co-transfer model

using OT-II TCR transgenic mice to assess antigen specific responses by infant OT-II cells compared to adult OT-II cells within individual host. OT-II cells were also stimulated with cognate antigen to assess antigen specific TCR signaling differences between infant and adult OT-II cells ex vivo. Human $CD4^+$ T cells from lymph nodes were also stimulated *ex vivo* to assess for enhanced T cell signal strength capacity.

Mice

Mice were housed and bred in specific pathogen-free (Spf) conditions in the animal facilities at Columbia University Irving Medical Center (CUIMC). Male and female OT-II (B6.Cg.Tg(TcraTcrb)425Cbn/J) (27) and CD45.1(B6.SJL-$Ptprc^aPepc^b$/BoyJ) mice were purchased from Jackson Laboratories while C57BL/6 mice were purchased from Charles River. Male TCF-1 transgenic (p45 - Tg) mice expressing the long isoform of TCF-1(33) were generously provided by Dr. Hai-Hui Xue and Dr. Werner Held. CD45.1 mice were bred to generate CD45.1 congenic hosts and CD45.2 mice were bred to use for phosphoflow studies. OT-II mice were also crossed to CD45.1 mice and TCF-1 Tg OT-II mice were generated by breeding TCF-1 Tg male to OT-II females. All infant mice were used at 10-14 days of age, and adult mice were used at 6 weeks and older. Infections were performed in BSL-2 level biocontainment animal facilities. All animal studies were approved by Columbia University IACUC.

T cell adoptive transfer and Influenza infection

To isolate $CD4^+$ T cells from infant and adult mice, spleen and lymph nodes were harvested from euthanized mice and processed to generate a single cell suspension. Briefly, organs were meshed through 100μm filter (Corning) and washed with PBS (Corning). Red blood cells were lysed using ACK lysis buffer (Gibco) for 3min before addition of PBS. Cells were washed twice with PBS, filtered through 70μm filter (Corning) and counted using trypan blue (Gibco). Single litters of at least 5 pups were combined to generate sufficient numbers of $CD4^+$ T cells for each experiment. $CD4^+$ T cells were purified by negative magnetic selection (Stemcell Technologies). For co-transfers, 250,000 cells in 100μl of PBS containing 1:1 ratio of adult and infant OT-II T cells were transferred into adult congenic B6 or CD45.1 host mice retro-orbitally one-day prior (day −1) to infection. For 4-day *in vivo* proliferation experiments, OT-II T cells were labeled with cell proliferation dye (CPD) as per the manufacturer's protocol (ThermoFisher) and 500,000 each of infant and adult T cells were transferred into host mice. At day 0, host mice were infected intranasally (i.n.) with 2000 $TCID_{50}$ of a recombinant PR8-OVA strain expressing the OVA323–339 peptide (sequence ISQAVHAAHAEINEAGR; provided by Dr. Paul Thomas, St. Jude Children's Research Hospital, Memphis, TN)(60).

Flow cytometry

Mediastinal lymph nodes and lungs were harvested at indicated days of infections and processed to generate single cell suspension as previously described (11, 61). Briefly, lungs were dissociated using gentleMACs lung protocol (Miltenyi) and then digested for 1hr in RPMI media containing Collagenase D (Sigma), DNase (Sigma) and Trypsin inhibitor (Sigma) at 37 degrees shaking incubator. After digestion, cells were washed twice with complete media and filtered through 100μm and 70μm filters (Corning) and then counted.

Draining LNs were prepared as described above in T cell adoptive transfer and Influenza infection section for single cell suspension. Flow cytometry gating scheme is shown for mouse cells (figure S1) and human cells (figure S6). A list of all antibodies used for flow cytometry in this study is shown for mouse cells (Table S3) and human cells (Table S4). In general, cells were first stained with surface markers at 30 min room temperature (RT) and an additional 30 min on ice. Cells were then fixed and permeabilized with Foxp3 fix/perm (Tonbo) before being stained for intracellular markers for 30 min on ice. For OT-II TCR specific tetramer staining, cells were incubated with I-A(b)$_{AAHAEINEA}$ tetramers (NIH Tetramer Core Facility, NTCF) in 50μl for 1hr in 37°C incubator before addition of other surface markers with additional 30 min at RT before fixation as described above. All flow cytometry samples were acquired using LSRII flow cytometer (BD) with FACSDiva software. All cell sorting were performed in BD Influx cell sorter. Data were analyzed using FSC Express (DeNovo software) and FlowJo LLC (BD).

Human donor samples

Human adult lymph nodes were obtained from deceased (brain dead) organ donors through an approved protocol and material transfer agreement with LiveOnNY as described (62). Human infant lymph nodes were obtained from deceased (brain dead) organ donors under the Human Atlas for Neonatal Development and Early Life – Immunity (HANDEL-I) tissue procurement program. A list of all donors used and their ages is in Table S1, and compiled ages and sex in Table S2. Tissues were obtained and processed for single-cell suspensions, as previously described (63). The study does not qualify as human subjects research as determined by Columbia University institutional review board (IRB), because tissue samples were obtained from deceased individuals.

Mouse T cell stimulations

For activation of OT-II CD4$^+$ T cells, OT-II cells were isolated from spleens and LNs of infant and adult mice as described above (T cell adoptive transfer and Influenza infection section), while antigen presenting cells (APC) were isolated by magnetic depletion of CD3$^+$ T cells (Miltenyi, as per manufacturer's protocol) from single cell suspension of total spleen cells. To deplete CD3$^+$ T cells, total splenoctyes were incubated with biotin anti-mouse CD3 (Biolegend) for 15min at room temperature then washed before incubating with anti-biotin microbeads (Miltenyi) for 15min on ice. Cells were magnetically sorted through an LS magnetic column where the flow through was collected as APCs. OT-II cells were labeled with eFlour450 proliferation dye (ThermoFisher, as per manufacturer's protocol) and cultured 1:1 with APCs from adult (7 weeks and older) or infant (10 – 14 days) CD45.1 or C57BL/6 mice in the presence of chicken ovalbumin peptide epitope recognized by the OT-II TCR (ISQAVHAAHAEINEAGR) (InVivoGen) in complete RPMI media (10% fetal bovine serum (FBS), 1% penicillin – streptomycin-glutamine (PSQ), 25mM HEPES). Controls were T cell and APC cultured without peptide. For short-term stimulations for assessing TCR signaling, infant or adult OT-II cells were stimulated with 10μg of peptide-pulsed T cell-depleted splenocytes. For measuring cytokine production by lung T cells, total lung cells were isolated as described (11, 61) from mice at day 11 post-infection and stimulated in the presence of 10μg of peptide for 16 hr in complete RPMI. Protein transport inhibitor cocktail (ThermoFisher) was added 2 hours into stimulation.

After stimulation, cells were first stained with surface markers, then fixed and permeabilized with Foxp3 fix/perm (Tonbo) before being stained for intracellular cytokine for 30 min on ice.

Human T cell stimulation

Naïve ($CD45RA^+CCR7^+$) $CD4^+$ T cells were sorted from lymph nodes (LN), labeled with cell proliferation dye (CPD), and allowed to rest overnight before stimulation. To sort naïve $CD4^+$ T cells, single cell suspension from lung LN or mesenteric LN were labeled with antibodies (fixable viable dye, CD45, CD4, CD8, CD45RA and CCR7; antibody information is provided in Supplemental material - Table S4) for 30min on ice. Cells were washed twice with FACS buffer, filtered through 40μm filter and then sorted using BD influx sorter. Sorted $CD4^+$ naïve T cells (100,000 cells/well) were cultured with carboxylate modified latex (CML) microbeads (ThermoFisher) functionalized with 10μg/mL of anti-CD28 (BioXcell) and anti-CD2 (ThermoFisher) monoclonal antibodies and 0.1 - 10μg/mL of anti-CD3 monoclonal antibody (BioXcell), at 1:1 in complete AIM V media (10% human serum, 1% PSQ, Glutamax, and IL-2 (50ng/ml)). Preparation of CML microbeads used for stimulation was done as described (64-66). To measure cytokine production, sorted $CD4^+$ T cells were stimulated for 4 days with beads in complete AIM V media before stimulation with PMA/ionomycin (Sigma) and protein transport inhibitor cocktail (ThermoFisher) for 6 hours. After stimulation, cells were first stained with surface markers, then fixed and permeabilized with Foxp3 fix/perm (Tonbo) before being stained for intracellular cytokine. For short-term (0-8hr) stimulation, total lymph node T cells were pre-stained with surface makers CD4, CD3, CD45RA, and CCR7 before being plated in complete RPMI media. Cells were stimulated using beads coated with 10μg/mL of anti-CD3/ anti-CD28/ anti-CD2 (Miltenyi) for indicated time. At each time point, cells were harvested and further stained for surface marker (CD3) before being fixed and permeabilized for intracellular marker Nur77.

TCR signaling analysis using Phosphoflow

C57BL/6 wild-type (WT) mice were used for examination of phosphoERK1/2 expression upon stimulation. Cells were isolated with magnetic negative enrichment using CD3 isolation kit (StemCell). CD3 enriched cells were kept ice cold until time of stimulation in 37°C water bath. Cells were first labeled with anti-CD3ε (10μg/ml) and anti-CD28 (5μg/ml) (BioXcell) antibodies in ice cold PBS for 30min on ice. Cells were washed and then stained with cross-linker goat anti-Armenian hamster IgG (Jackson Immuno Research Laboratories) (20μg/ml) and anti-CD44/ anti-CD62L antibodies for additional 30min on ice. Tubes were then placed in water bath to start stimulation and lyse/fix buffer (BD) was added to stop stimulation at indicated times. Cells were permeabilized with Perm III buffer (BD) before being stained for CD3, CD4, CD8, and pERK1/2. Samples were acquired in LSRII cytometer and analyzed using Flowjo software.

Analysis of T cell and APC conjugates

To image immunological synapse (IS) formation between OT-II T cells and APC, CPD labeled OT-II cells were pre-stained with anti-CD4 antibodies at 4°C and washed with ice cold PBS before stimulation. APCs were isolated as described above (mouse T cell stimulation *section*) and then labeled with CFSE (ThermoFisher). Briefly, 20 million APCs

in 1ml 1x PBS were incubated with 1ml of 1x PBS containing CFSE dye for 10min in 37 degrees before ice cold complete media was added. Cells were rested for 5min on ice before spinning down and washed twice with complete media. OT-II cells were then placed with 0.1μg – 10μg of peptide pulsed T cell-depleted CFSE-labeled splenocytes and spun down at 100 x g for 1min to enable conjugation. Stimulation was started by placing tubes into 37°C water bath. After each stimulation time point, cells were fixed with cytofix (BD) and placed on ice overnight. The next day cells were washed and then permeabilized with 1x Triton-X solution (Sigma-Aldrich) for 15min RT. After wash, cells were stained with the rest of the markers for 45min at RT before being analyzed by ImageStream X (Amnis, Seattle, WA).

ImageStream analysis

Images were acquired at 60x magnification on a four-laser ImageStream X (Amnis, Seattle, WA) imaging flow cytometer with INSPIRE software. Data was analyzed using IDEAS v6. Using Area measurement, doublet cells were gated and acquired for all samples. From doublet cells, events with both CPD and CFSE dye were gated to identify conjugates of T cell:APC. Previously published analysis from Au-Wabnitz et al and Abrahamsen et al was adapted (46, 47). Using the ‘threshold’ mask function on CPD channel, T cell were highlighted. With ‘interface’ mask function on CPD, the immune synapse of T cells was highlighted. Formula used to quantify accumulation of molecules in the IS:

$$\text{percent accumulation} = \frac{\text{intensity in IS}}{\text{intensity in T cell}} \times 100$$

To measure co-localization of CD4 and lck with CD3 (figure S5D), ‘bright detail colocalization 3’ (BDC) feature was used:

$$\text{percent co-localization of 3 molecules} = \frac{\text{BDC in IS}}{\text{BDC in T cell}} \times 100$$

To measure co-localization of two markers of interest (figure S5C & D), ‘bright detail similar R3’ (BDS) feature was used:

$$\text{percent co-localization of 2 molecules} = \frac{\text{BDS in IS}}{\text{BDS in T cell}} \times 100$$

To adjust for background differences existing before stimulation, quantification was normalized to unstimulated controls.

Statistical analysis

All data were compiled, and statistical analysis performed using Prism software (GraphPad Software). Each connected dot represents infant and adult cells from an individual host. Results are shown with SEM unless otherwise indicated. Significance was determined using either paired or unpaired Student’s *t*-test (2-tailed), or two-way repeated measure ANOVA with multiple comparison testing using the Sidak method, or one-way ANOVA with Tukey multiple comparison testing. Result was designated significant when p value was $p \leq 0.05$. The paired T test was used for direct comparison of adult and infant T cells in the same

host (Figs. 1-3). For side-by-side comparison of infant and adult T cells in *ex vivo* dose and kinetic responses (Fig. 4, 5, 6, 7), we used two-way ANOVA with multiple comparison because we are measuring 2 independent variables (adult vs infant and time) in combination for quantifying T cell activation and proliferation. All experiments were performed at least twice. Host mice were challenged intranasally (i.n.) with PR8-OVA. For co-transfer mice experiments at least three biological replicates (three individual host mice) were used in each experiment. A biological replicate was excluded only if donor OT-II cells were absent in both lungs and medLN of individual host which was considered a technical failure and occurred rarely.

Supplementary Material

Refer to Web version on PubMed Central for supplementary material.

Acknowledgements

We are grateful to Werner Held, University of Lausanne, and Hai-Hui Xue, University of Iowa, for their generosity in providing the TCF-1 (p45) Tg mice. We wish to thank the NIH Tetramer Core Facility (NTCF) for providing I-A(b)$_{AAHAEINEA}$ tetramers. We wish to thank Stuart Weisberg for reviewing the manuscript and his helpful comments and discussion.

Funding

This work was supported by NIH grants AI100119, AI106697 awarded to D.L.F. T.J.C. was supported by K23 AI141686 and T.M.B was supported by AI42288. These studies were performed in the CCTI Flow Cytometry Core supported by NIH S10RR027050 and S10OD020056. Acquisition of human samples from the University of Florida was supported by the Helmsley Charitable Trust (to T.M.B. and D.L.F.) ImageStream experiments were performed in Columbia Stem Cell initiative (CSCI) Flow Core, supported in part by NIH (S10OD026845).

References and notes

1. Mohr E, Siegrist C-A, Vaccination in early life: standing up to the challenges. Current Opinion in Immunology 41, 1–8 (2016). [PubMed: 27104290]
2. PrabhuDas M, Adkins B, Gans H, King C, Levy O, Ramilo O, Siegrist CA, Challenges in infant immunity: implications for responses to infection and vaccines. Nat Immunol 12, 189–194 (2011). [PubMed: 21321588]
3. Alsohime F, Temsah M-H, Al-Nemri AM, Somily AM, Al-Subaie S, COVID-19 infection prevalence in pediatric population: Etiology, clinical presentation, and outcome. J Infect Public Health 13, 1791–1796 (2020). [PubMed: 33127335]
4. Barrero-Castillero A, Beam KS, Bernardini LB, Ramos EGC, Davenport PE, Duncan AR, Fraiman YS, Frazer LC, Healy H, Herzberg EM, Keyes ML, Leeman KT, Leone K, Levin JC, Lin M, Raju RM, Sullivan A, C.-W. G. On behalf of the Harvard Neonatal-Perinatal Fellowship, COVID-19: neonatal–perinatal perspectives. Journal of Perinatology, (2020).
5. Alexander-Miller MA, Challenges for the Newborn Following Influenza Virus Infection and Prospects for an Effective Vaccine. Frontiers in immunology 11, 568651–568651 (2020). [PubMed: 33042150]
6. PrabhuDas M, Adkins B, Gans H, King C, Levy O, Ramilo O, Siegrist C-A, Challenges in infant immunity: implications for responses to infection and vaccines. Nature Immunology 12, 189–194 (2011). [PubMed: 21321588]
7. Schmiedeberg K, Krause H, Röhl F-W, Hartig R, Jorch G, Brunner-Weinzierl MC, T Cells of Infants Are Mature, but Hyporeactive Due to Limited Ca2+ Influx. PloS one 11, e0166633–e0166633 (2016). [PubMed: 27893767]

8. Pichichero ME, Casey JR, Almudevar A, Basha S, Surendran N, Kaur R, Morris M, Livingstone AM, Mosmann TR, Functional Immune Cell Differences Associated With Low Vaccine Responses in Infants. The Journal of Infectious Diseases 213, 2014–2019 (2016). [PubMed: 26908730]
9. Davenport MP, Smith NL, Rudd BD, Building a T cell compartment: how immune cell development shapes function. Nat Rev Immunol 20, 499–506 (2020). [PubMed: 32493982]
10. Rudd BD, Neonatal T Cells: A Reinterpretation. Annu Rev Immunol 38, 229–247 (2020). [PubMed: 31928469]
11. Zens KD, Chen JK, Guyer RS, Wu FL, Cvetkovski F, Miron M, Farber DL, Reduced generation of lung tissue-resident memory T cells during infancy. The Journal of experimental medicine 214, 2915–2932 (2017). [PubMed: 28855242]
12. Smith NL, Wissink E, Wang J, Pinello JF, Davenport MP, Grimson A, Rudd BD, Rapid proliferation and differentiation impairs the development of memory CD8+ T cells in early life. J Immunol 193, 177–184 (2014). [PubMed: 24850719]
13. Adkins B, Bu Y, Guevara P, The generation of Th memory in neonates versus adults: prolonged primary Th2 effector function and impaired development of Th1 memory effector function in murine neonates. J Immunol 166, 918–925 (2001). [PubMed: 11145668]
14. Smith NL, Patel RK, Reynaldi A, Grenier JK, Wang J, Watson NB, Nzingha K, Yee Mon KJ, Peng SA, Grimson A, Davenport MP, Rudd BD, Developmental Origin Governs CD8+ T Cell Fate Decisions during Infection. Cell 174, 117–130.e114 (2018). [PubMed: 29909981]
15. Joshi NS, Cui W, Chandele A, Lee HK, Urso DR, Hagman J, Gapin L, Kaech SM, Inflammation directs memory precursor and short-lived effector CD8(+) T cell fates via the graded expression of T-bet transcription factor. Immunity 27, 281–295 (2007). [PubMed: 17723218]
16. Zhou X, Yu S, Zhao DM, Harty JT, Badovinac VP, Xue HH, Differentiation and persistence of memory CD8(+) T cells depend on T cell factor 1. Immunity 33, 229–240 (2010). [PubMed: 20727791]
17. Yu Q, Sharma A, Oh SY, Moon HG, Hossain MZ, Salay TM, Leeds KE, Du H, Wu B, Waterman ML, Zhu Z, Sen JM, T cell factor 1 initiates the T helper type 2 fate by inducing the transcription factor GATA-3 and repressing interferon-gamma. Nat Immunol 10, 992–999 (2009). [PubMed: 19648923]
18. Nish SA, Zens KD, Kratchmarov R, Lin WW, Adams WC, Chen YH, Yen B, Rothman NJ, Bhandoola A, Xue HH, Farber DL, Reiner SL, CD4+ T cell effector commitment coupled to self-renewal by asymmetric cell divisions. J Exp Med 214, 39–47 (2017). [PubMed: 27923906]
19. Monks CRF, Freiberg BA, Kupfer H, Sciaky N, Kupfer A, Three-dimensional segregation of supramolecular activation clusters in T cells. Nature 395, 82–86 (1998). [PubMed: 9738502]
20. Dustin ML, Cooper JA, The immunological synapse and the actin cytoskeleton: molecular hardware for T cell signaling. Nature Immunology 1, 23–29 (2000). [PubMed: 10881170]
21. Grakoui A, Bromley SK, Sumen C, Davis MM, Shaw AS, Allen PM, Dustin ML, The Immunological Synapse: A Molecular Machine Controlling T Cell Activation. Science 285, 221 (1999). [PubMed: 10398592]
22. Li Q-J, Dinner AR, Qi S, Irvine DJ, Huppa JB, Davis MM, Chakraborty AK, CD4 enhances T cell sensitivity to antigen by coordinating Lck accumulation at the immunological synapse. Nature Immunology 5, 791–799 (2004). [PubMed: 15247914]
23. Straus DB, Weiss A, Genetic evidence for the involvement of the lck tyrosine kinase in signal transduction through the T cell antigen receptor. Cell 70, 585–593 (1992). [PubMed: 1505025]
24. King Carolyn G., Koehli S, Hausmann B, Schmaler M, Zehn D, Palmer E, T Cell Affinity Regulates Asymmetric Division, Effector Cell Differentiation, and Tissue Pathology. Immunity 37, 709–720 (2012). [PubMed: 23084359]
25. Cho Y-L, Flossdorf M, Kretschmer L, Höfer T, Busch DH, Buchholz VR, TCR Signal Quality Modulates Fate Decisions of Single CD4+ T Cells in a Probabilistic Manner. Cell Reports 20, 806–818 (2017). [PubMed: 28746867]
26. Snook JP, Kim C, Williams MA, TCR signal strength controls the differentiation of CD4(+) effector and memory T cells. Sci Immunol 3, (2018).

27. Barnden MJ, Allison J, Heath WR, Carbone FR, Defective TCR expression in transgenic mice constructed using cDNA-based α- and β-chain genes under the control of heterologous regulatory elements. Immunology & Cell Biology 76, 34–40 (1998). [PubMed: 9553774]
28. Paik DH, Farber DL, Influenza infection fortifies local lymph nodes to promote lung-resident heterosubtypic immunity. Journal of Experimental Medicine 218, (2020).
29. Ho AW, Prabhu N, Betts RJ, Ge MQ, Dai X, Hutchinson PE, Lew FC, Wong KL, Hanson BJ, Macary PA, Kemeny DM, Lung CD103+ dendritic cells efficiently transport influenza virus to the lymph node and load viral antigen onto MHC class I for presentation to CD8 T cells. J Immunol 187, 6011–6021 (2011). [PubMed: 22043017]
30. Lin W-HW, Nish SA, Yen B, Chen Y-H, Adams WC, Kratchmarov R, Rothman NJ, Bhandoola A, Xue H-H, Reiner SL, CD8(+) T Lymphocyte Self-Renewal during Effector Cell Determination. Cell reports 17, 1773–1782 (2016). [PubMed: 27829149]
31. Szabo SJ, Kim ST, Costa GL, Zhang X, Fathman CG, Glimcher LH, A Novel Transcription Factor, T-bet, Directs Th1 Lineage Commitment. Cell 100, 655–669 (2000). [PubMed: 10761931]
32. Danilo M, Chennupati V, Silva JG, Siegert S, Held W, Suppression of Tcf1 by Inflammatory Cytokines Facilitates Effector CD8 T Cell Differentiation. Cell Reports 22, 2107–2117 (2018). [PubMed: 29466737]
33. Ioannidis V, Beermann F, Clevers H, Held W, The β-catenin–TCF-1 pathway ensures CD4+CD8+ thymocyte survival. Nature Immunology 2, 691–697 (2001). [PubMed: 11477404]
34. Gallegos AM, Xiong H, Leiner IM, Sušac B, Glickman MS, Pamer EG, van Heijst JWJ, Control of T cell antigen reactivity via programmed TCR downregulation. Nature Immunology 17, 379–386 (2016). [PubMed: 26901151]
35. Landais E, Romagnoli PA, Corper AL, Shires J, Altman JD, Wilson IA, Garcia KC, Teyton L, New Design of MHC Class II Tetramers to Accommodate Fundamental Principles of Antigen Presentation. The Journal of Immunology 183, 7949 (2009). [PubMed: 19923463]
36. Ashouri JF, Weiss A, Endogenous Nur77 Is a Specific Indicator of Antigen Receptor Signaling in Human T and B Cells. The Journal of Immunology, 1601301 (2016).
37. Cunningham NR, Artim SC, Fornadel CM, Sellars MC, Edmonson SG, Scott G, Albino F, Mathur A, Punt JA, Immature CD4+CD8+ thymocytes and mature T cells regulate Nur77 distinctly in response to TCR stimulation. J Immunol 177, 6660–6666 (2006). [PubMed: 17082578]
38. Nayar R, Schutten E, Bautista B, Daniels K, Prince AL, Enos M, Brehm MA, Swain SL, Welsh RM, Berg LJ, Graded levels of IRF4 regulate CD8+ T cell differentiation and expansion, but not attrition, in response to acute virus infection. J Immunol 192, 5881–5893 (2014). [PubMed: 24835398]
39. Moran AE, Holzapfel KL, Xing Y, Cunningham NR, Maltzman JS, Punt J, Hogquist KA, T cell receptor signal strength in Treg and iNKT cell development demonstrated by a novel fluorescent reporter mouse. The Journal of experimental medicine 208, 1279–1289 (2011). [PubMed: 21606508]
40. Nayar R, Enos M, Prince A, Shin H, Hemmers S, Jiang JK, Klein U, Thomas CJ, Berg LJ, TCR signaling via Tec kinase ITK and interferon regulatory factor 4 (IRF4) regulates CD8+ T-cell differentiation. Proc Natl Acad Sci U S A 109, E2794–2802 (2012). [PubMed: 23011795]
41. Delgado P, Fernández E, Dave V, Kappes D, Alarcón B, CD3δ couples T-cell receptor signalling to ERK activation and thymocyte positive selection. Nature 406, 426–430 (2000). [PubMed: 10935641]
42. Dustin ML, T-cell activation through immunological synapses and kinapses. Immunological Reviews 221, 77–89 (2008). [PubMed: 18275476]
43. Ryser JE, Rungger-Brändle E, Chaponnier C, Gabbiani G, Vassalli P, The area of attachment of cytotoxic T lymphocytes to their target cells shows high motility and polarization of actin, but not myosin. The Journal of Immunology 128, 1159 (1982). [PubMed: 7035558]
44. Cambi A, Joosten B, Koopman M, de Lange F, Beeren I, Torensma R, Fransen JA, Garcia-Parajó M, van Leeuwen FN, Figdor CG, Organization of the Integrin LFA-1 in Nanoclusters Regulates Its Activity. Molecular Biology of the Cell 17, 4270–4281 (2006). [PubMed: 16855029]

45. Roy NH, Kim SHJ, Buffone A, Blumenthal D, Huang B, Agarwal S, Schwartzberg PL, Hammer DA, Burkhardt JK, LFA-1 signals to promote actin polymerization and upstream migration in T cells. Journal of Cell Science 133, jcs248328 (2020). [PubMed: 32907931]
46. Wabnitz G, Kirchgessner H, Samstag Y, Qualitative and Quantitative Analysis of the Immune Synapse in the Human System Using Imaging Flow Cytometry. JoVE, e55345 (2019).
47. Abrahamsen G, Sundvold-Gjerstad V, Habtamu M, Bogen B, Spurkland A, Polarity of CD4+ T cells towards the antigen presenting cell is regulated by the Lck adapter TSAd. Sci Rep 8, 13319–13319 (2018). [PubMed: 30190583]
48. Hartl FA, Beck-Garcìa E, Woessner NM, Flachsmann LJ, Cárdenas RMHV, Brandl SM, Taromi S, Fiala GJ, Morath A, Mishra P, Yousefi OS, Zimmermann J, Hoefflin N, Köhn M, Wöhrl BM, Zeiser R, Schweimer K, Günther S, Schamel WW, Minguet S, Noncanonical binding of Lck to CD3ε promotes TCR signaling and CAR function. Nature Immunology 21, 902–913 (2020). [PubMed: 32690949]
49. Roh K-H, Lillemeier BF, Wang F, Davis MM, The coreceptor CD4 is expressed in distinct nanoclusters and does not colocalize with T-cell receptor and active protein tyrosine kinase p56lck. Proceedings of the National Academy of Sciences 112, E1604 (2015).
50. Rossy J, Owen DM, Williamson DJ, Yang Z, Gaus K, Conformational states of the kinase Lck regulate clustering in early T cell signaling. Nature Immunology 14, 82–89 (2013). [PubMed: 23202272]
51. Wei Q, Brzostek J, Sankaran S, Casas J, Hew LS-Q, Yap J, Zhao X, Wojciech L, Gascoigne NRJ, Lck bound to coreceptor is less active than free Lck. Proceedings of the National Academy of Sciences 117, 15809 (2020).
52. Blumenthal D, Burkhardt JK, Multiple actin networks coordinate mechanotransduction at the immunological synapse. Journal of Cell Biology 219, (2020).
53. Zens KD, Chen JK, Guyer RS, Wu FL, Cvetkovski F, Miron M, Farber DL, Reduced generation of lung tissue-resident memory T cells during infancy. J Exp Med 214, 2915–2932 (2017). [PubMed: 28855242]
54. Opiela SJ, Koru-Sengul T, Adkins B, Murine neonatal recent thymic emigrants are phenotypically and functionally distinct from adult recent thymic emigrants. Blood 113, 5635–5643 (2009). [PubMed: 19168791]
55. Fink PJ, Hendricks DW, Post-thymic maturation: young T cells assert their individuality. Nature Reviews Immunology 11, 544–549 (2011).
56. Dong M, Artusa P, Kelly SA, Fournier M, Baldwin TA, Mandl JN, Melichar HJ, Alterations in the Thymic Selection Threshold Skew the Self-Reactivity of the TCR Repertoire in Neonates. J Immunol 199, 965–973 (2017). [PubMed: 28659353]
57. Ruckwardt TJ, Malloy AM, Gostick E, Price DA, Dash P, McClaren JL, Thomas PG, Graham BS, Neonatal CD8 T-cell hierarchy is distinct from adults and is influenced by intrinsic T cell properties in respiratory syncytial virus infected mice. PLoS Pathog 7, e1002377 (2011). [PubMed: 22144888]
58. Weisberg SP, Connors TJ, Zhu Y, Baldwin MR, Lin W-H, Wontakal S, Szabo PA, Wells SB, Dogra P, Gray J, Idzikowski E, Stelitano D, Bovier FT, Davis-Porada J, Matsumoto R, Poon MML, Chait M, Mathieu C, Horvat B, Decimo D, Hudson KE, Zotti FD, Bitan ZC, La Carpia F, Ferrara SA, Mace E, Milner J, Moscona A, Hod E, Porotto M, Farber DL, Distinct antibody responses to SARS-CoV-2 in children and adults across the COVID-19 clinical spectrum. Nature Immunology 22, 25–31 (2021). [PubMed: 33154590]
59. Richer MJ, Nolz JC, Harty JT, Pathogen-specific inflammatory milieux tune the antigen sensitivity of CD8(+) T cells by enhancing T cell receptor signaling. Immunity 38, 140–152 (2013). [PubMed: 23260194]
60. Thomas PG, Brown SA, Morris MY, Yue W, So J, Reynolds C, Webby RJ, Doherty PC, Physiological numbers of CD4+ T cells generate weak recall responses following influenza virus challenge. J Immunol 184, 1721–1727 (2010). [PubMed: 20061406]
61. Turner DL, Bickham KL, Thome JJ, Kim CY, D'Ovidio F, Wherry EJ, Farber DL, Lung niches for the generation and maintenance of tissue-resident memory T cells. Mucosal Immunol 7, 501–510 (2014). [PubMed: 24064670]

62. Thome Joseph J. C., Yudanin N, Ohmura Y, Kubota M, Grinshpun B, Sathaliyawala T, Kato T, Lerner H, Shen Y, Farber Donna L., Spatial Map of Human T Cell Compartmentalization and Maintenance over Decades of Life. Cell 159, 814–828 (2014). [PubMed: 25417158]

63. Sathaliyawala T, Kubota M, Yudanin N, Turner D, Camp P, Thome Joseph J. C., Bickham Kara L., Lerner H, Goldstein M, Sykes M, Kato T, Farber Donna L., Distribution and Compartmentalization of Human Circulating and Tissue-Resident Memory T Cell Subsets. Immunity 38, 187–197 (2013). [PubMed: 23260195]

64. Schrum AG, Visualization of Multiprotein Complexes by Flow Cytometry. Current Protocols in Immunology 87, 5.9.1–5.9.14 (2009).

65. Reed BK, Chopp LB, Malo CS, Renner DN, Van Keulen VS, Girtman MA, Nevala WN, Pavelko KD, Gil D, Schrum AG, Johnson AJ, Pease LR, A Versatile Simple Capture Assay for Assessing the Structural Integrity of MHC Multimer Reagents. PLOS ONE 10, e0137984 (2015). [PubMed: 26389800]

66. Schrum AG, Gil D, Dopfer EP, Wiest DL, Turka LA, Schamel WW, Palmer E, High-sensitivity detection and quantitative analysis of native protein-protein interactions and multiprotein complexes by flow cytometry. Sci STKE 2007, pl2 (2007). [PubMed: 17551170]

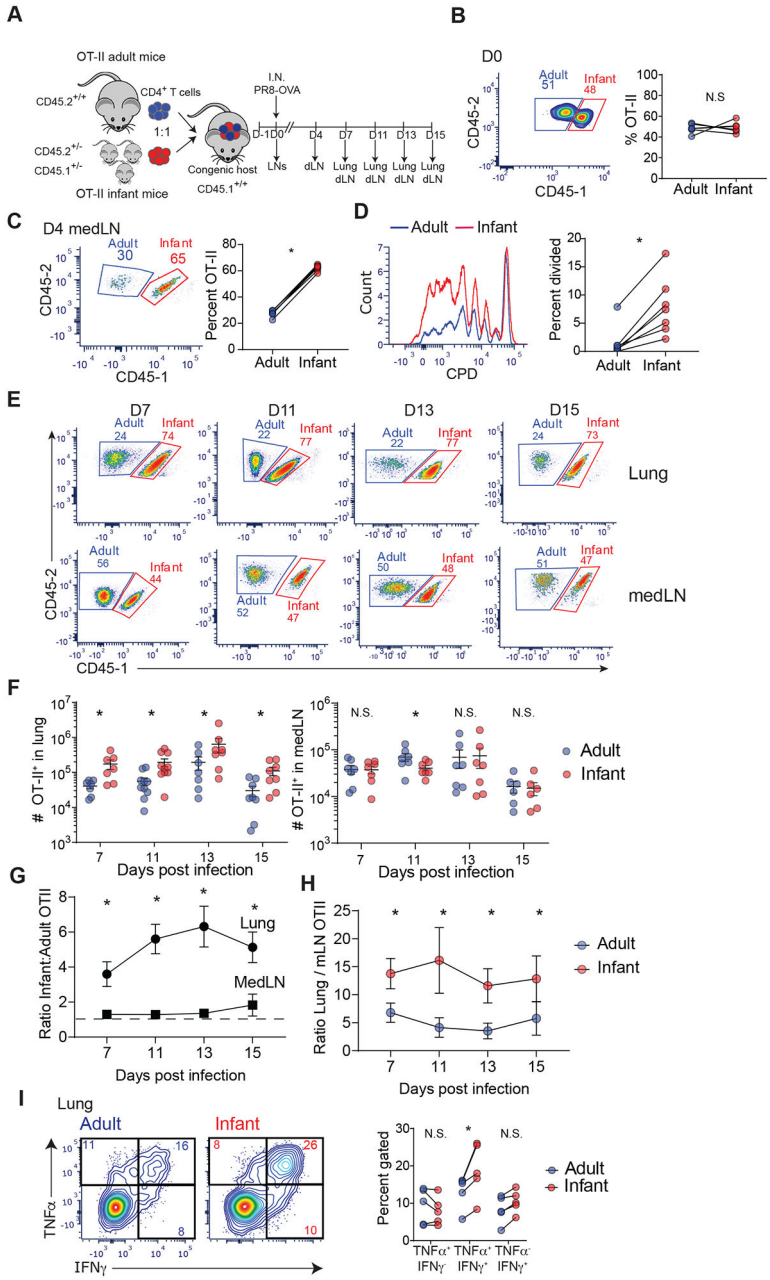

Fig. 1: Enhanced generation of lung-homing effector cells by infant compared to adult T cells during influenza virus infection.

(A) Schematic diagram depicting model for co-transfer of infant (red) and adult (blue) OT-II T cells into congenic host mice (CD45.2$^{-/-}$ CD45.1$^{+/+}$), followed by infection with PR8-OVA, and tissue harvest at indicated days post challenge. dLN, lung-draining (mediastinal) lymph node. **(B)** Frequency of transferred infant CD45.1^{+} (red) and adult CD45.1^{-} (blue) OT-II cells in LNs of host mice shown in representative flow cytometry plots (left) and in graphs of paired frequencies within individual host mice (right). **(C)** MedLN T cells at day 4 post infection (p.i.) shown in representative flow cytometry plots (left) and graph with paired frequencies (right) of infant and adult OT-II cells in individual host mice. **(D)** Proliferation

by infant OT-II cells relative to adult OT-II cells in medLN shown by flow cytometry plots of CPD dilution (left) and paired frequencies of divided infant (red) and adult (blue) OT-II cells (right) in individual host mice. **(E)**Representative flow cytometry plots showing frequency of infant (red) and adult (blue) OT-II cells from lungs and medLN of congenic hosts at indicated days post-infection. **(F)** Graphs showing total number of infant (red) and adult (blue) OT-II cells in lung (left) and medLN (right) of individual host at indicated days post infection. **(G)** Ratio of infant to adult OT-II cell numbers in lung and medLN of congenic hosts post infection. **(H)** Ratio of OT-II cells in lung:medLN from adult or infant in congenic hosts post infection derived from cell numbers. **(I)** Cytokine production by lung effector OT-II cells shown in representative flow plots of IFN-γ and TNF-α by infant and adult OT-II cells (left) and in graphs of paired frequencies of OT-II cells producing indicated cytokines from individual host mice (right). Lung effector T cells at day 11 p.i. were stimulated with 10 μg of peptide for 16 hours and examined for cytokine production. Each connected dot represents infant and adult from an individual host. Data are representative of at least 2 independent experiments with n = 3-4 mice per experiment. Statistical analysis was done using Student's paired t-test (*$p<0.05$) with error bars representing standard error mean (S.E.M.).

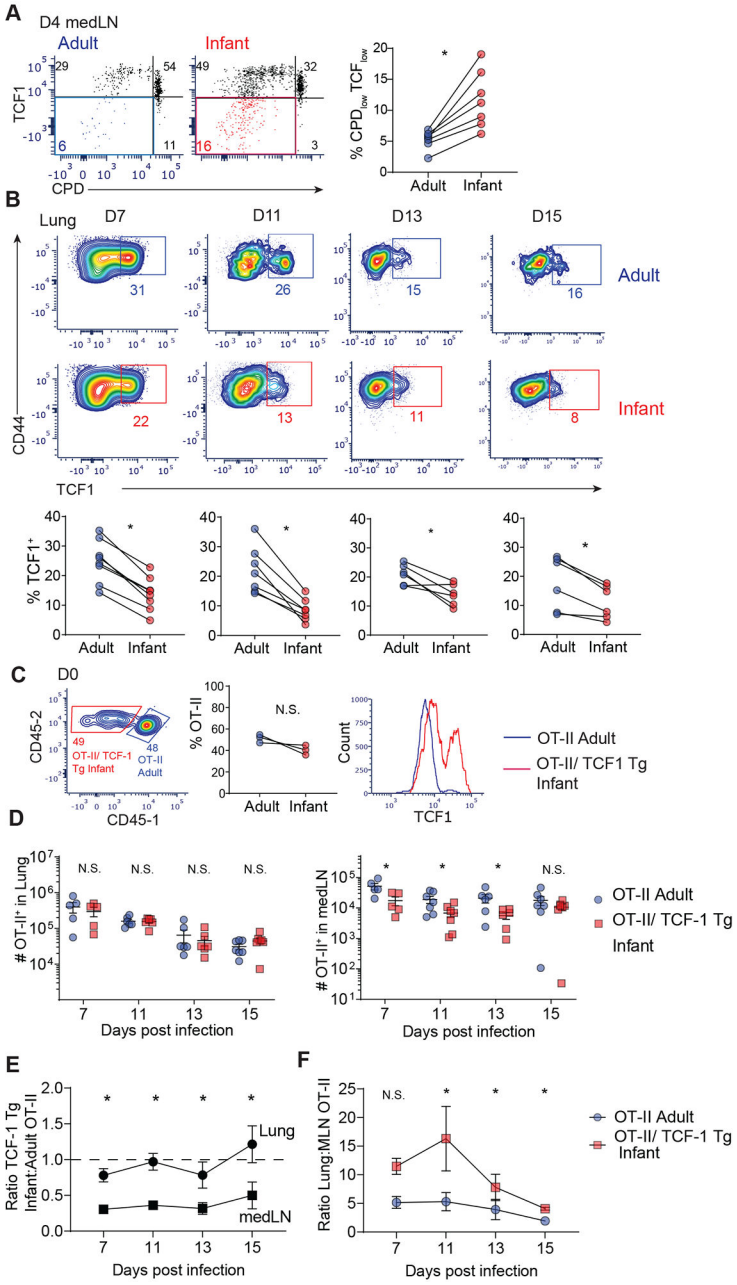

Fig. 2: Role of TCF-1 in enhanced proliferation of infant T cells.

(A) Expression of TCF-1 as a function of proliferation (CPD expression) at day 4 post infection in medLN of host mice shown in flow cytometry plots (left) and graphs of paired frequencies of CPD_{low} TCF_{low} infant and adult OT-II cells (right). **(B)** TCF-1 expression shown in flow cytometry plots (top) and graphs (bottom) of individual paired frequencies of TCF-1^+ infant (red) and adult (blue) lung effector cells. **(C)** Left: Representative flow cytometry plots of transferred infant OT-II/TCF-1 Tg CD45.1^- (red) and adult CD45.1^+ (blue) OT-II cells in LNs of host mice at day 0. Middle: Paired frequencies of infant and adult OT-II cells within individual host mice. Right: Baseline expression of TCF-1 in OT-II/ TCF-1 Tg infant (red) compared to adult (blue) cells in LNs at day 0. **(D)** Total number of

OT-II/TCF-1 Tg infant (red) and OT-II adult (blue) cells in lung (left) and medLN (right) of individual mice at indicated days p.i.**(E)** Ratio of infant OT-II/TCF-1 Tg cells:adult OT-II cell numbers in lung and medLN of congenic hosts post infection. **(F)** Ratio of OT-II in lung:medLN from OT-II adult or OT-II/ TCF-1 Tg infant in congenic hosts post infection derived from cell numbers. Data are representative of 2 independent experiments with n=3-4 mice per experiment. Statistical analysis was done using Student's paired t-test (*$p<0.05$) with error bars representing S.E.M.

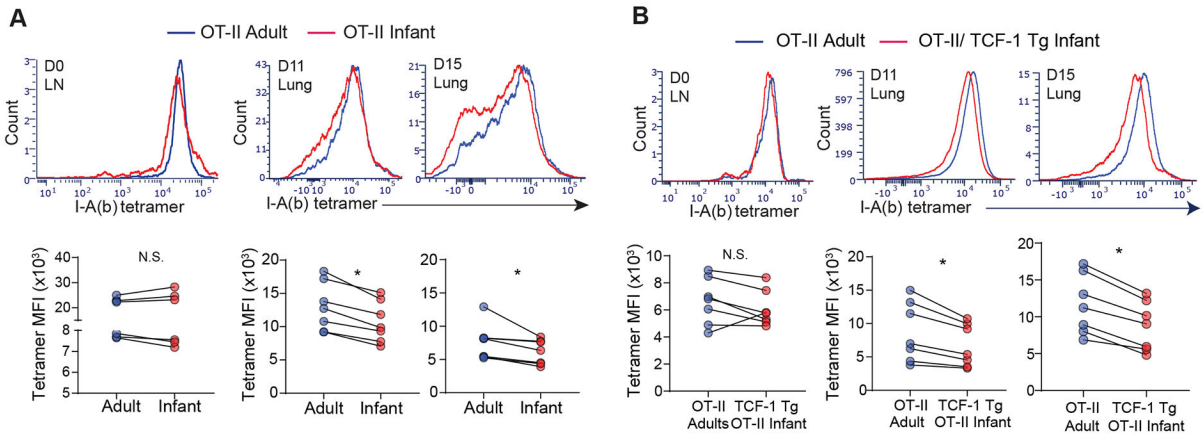

Fig. 3: Infant T cells exhibit features of enhanced TCR-mediated signaling during influenza responses *in vivo*.

(A) Expression of OT-II TCR using I-A(b)$_{AAHAEINEA}$ tetramer on infant (red) and adult (blue) OT-II cells from LNs and lungs at indicated day p.i. shown in histograms (top) and graphs with mean fluorescent intensity (MFI) of I-A(b) tetramer (bottom). **(B)** Expression of OT-II TCR on lung infant OT-II/TCF-1 Tg and adult OT-II effector cells shown in representative flow cytometry plots (top) and graphs quantifying MFI of tetramer (bottom) of individual hosts. Data are representative of 2 independent experiments with n = 3-4 mice per experiment. Statistical analysis was done using Student's paired t-test (*p<0.05) with error bars representing S.E.M.

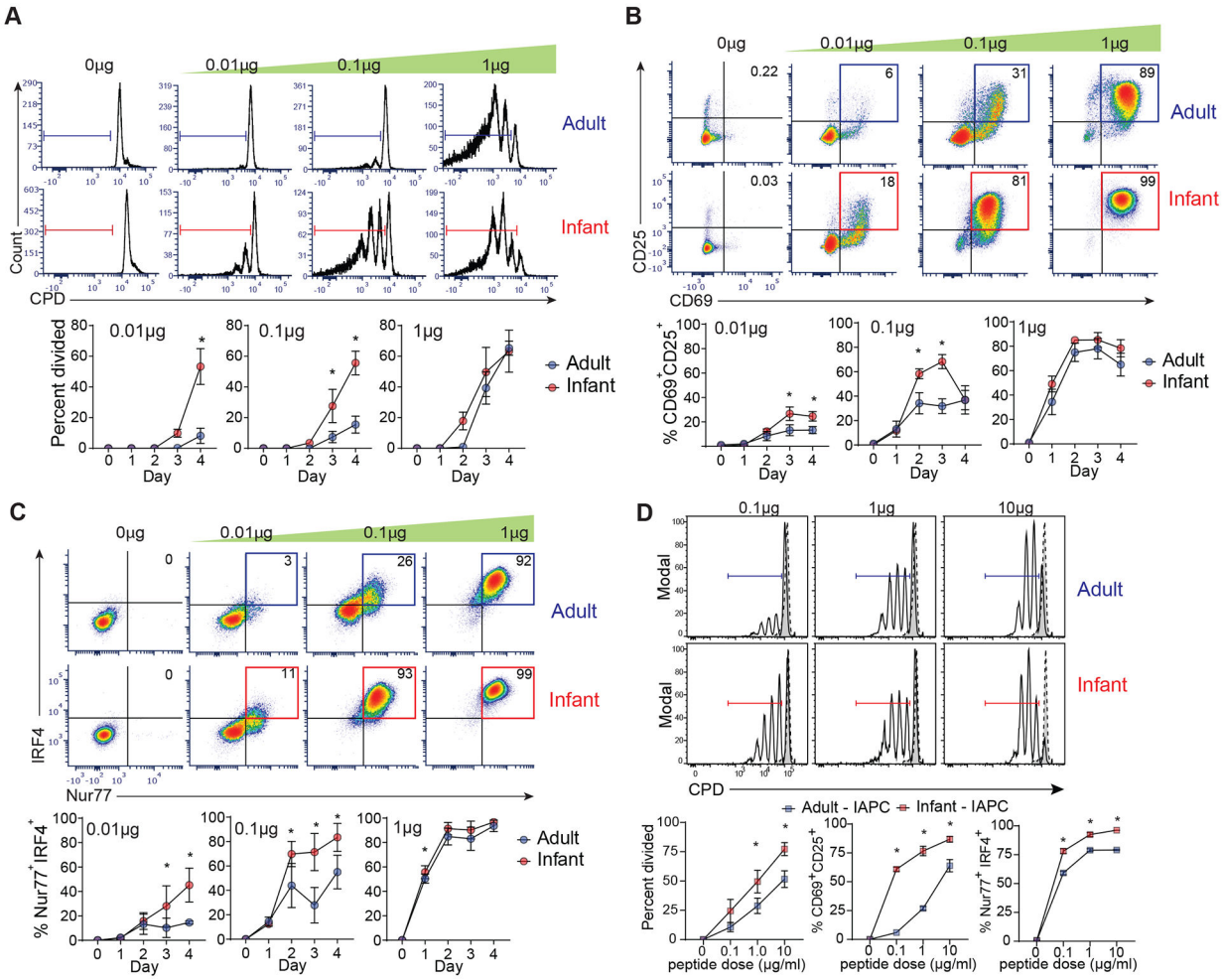

Fig. 4: Infant T cells have enhanced TCR sensitivity leading to decreased activation threshold.

Infant and adult OT-II cells were co-cultured with APC in different doses of ovalbumin peptide and harvested at 1-4 days post-stimulation **(A)** Proliferation of infant and adult OT-II cells to different antigen doses at day 3 post-stimulation shown in representative CPD dilution plots (top) and graphs quantifying percent divided at 1-4 days post-stimulation (bottom). Expression of CD69 and CD25 **(B)** and Nur77 and IRF4 **(C)** on infant and adult OT-II cells at day 3 post stimulation shown in representative flow cytometry plots (top) and graphs showing percent of $CD69^{+}CD25^{+}$ or $Nur77^{+}IRF4^{+}$ cells or for each dose over time (bottom). **(D)** (Top) Proliferation of infant and adult OT-II cells (black line) upon stimulation with infant antigen presenting cells (I-APC) at indicated peptide doses compared to unstimulated (dotted line). (Bottom) Expression of activation $CD69^{+}$ $CD25^{+}$, and percent $Nur77^{+}$ $IRF4^{+}$ expression by infant (red) and adult (blue) OT-II cells after 3 days of stimulation with I-APC at indicated doses. Data are compiled from 4 **(A-C)** and 2 **(D)** independent experiments. Statistical analysis was done using two-way ANOVA with Sidak multiple comparison testing.

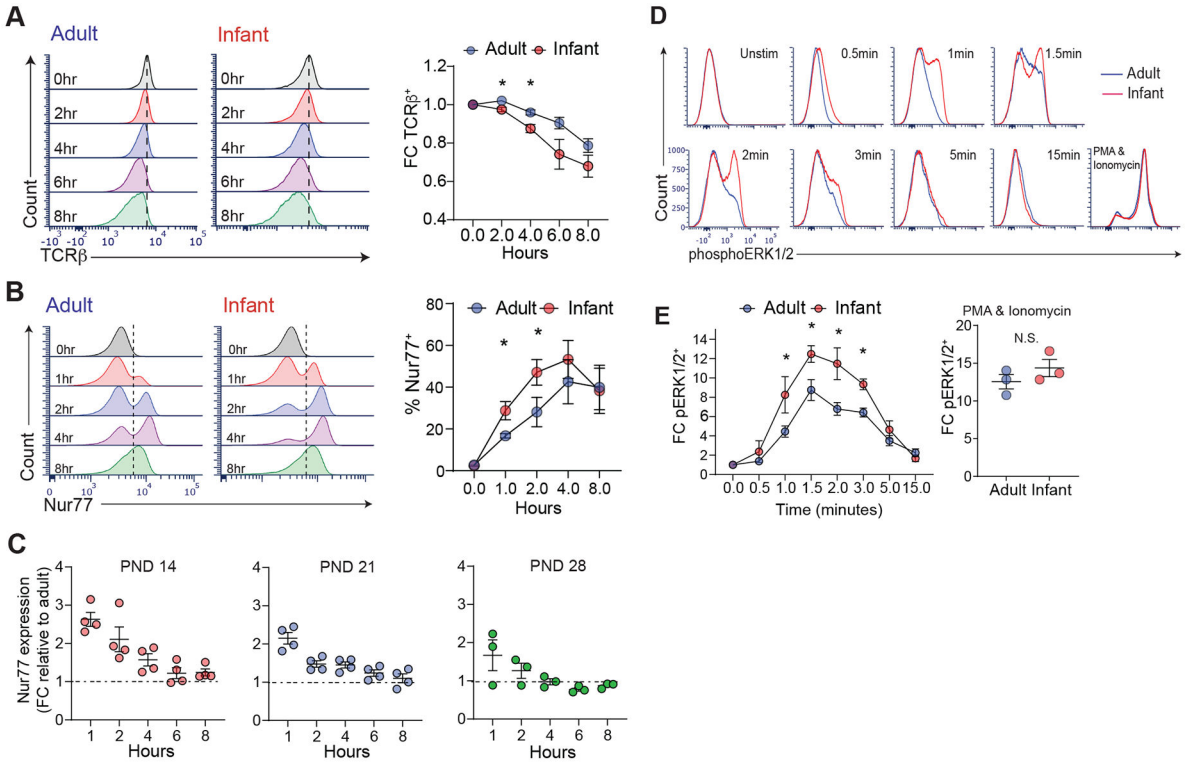

Fig. 5: Increased proximal signaling by infant compared to adult T cells.

Infant and adult OT-II cells were stimulated with ovalbumin-peptide (10μg) pulsed APCs for 0-8hrs. **(A)** Expression of surface TCR-β by infant (red) and adult (adult) OT-II cells shown in representative histograms (left) and graph showing fold change (FC) expression of TCR-β (bottom) upon antigen stimulation relative to unstimulated control. **(B)** Expression of Nur77 by infant and adult OT-II cells shown in flow cytometry plots (left) and graphs of percent Nur77^{+} (right) in OT-II cells at indicated times post-stimulation. Significance was determined using paired Student's *t*-test. **(C)** Expression of Nur77 shown as fold-change (FC) relative to adult (over 8 weeks) in OT-II cells derived from mice postnatal day (PND) 14, 21, and 28 as indicated upon stimulation with 10μg peptide pulsed APC for indicated times. **(D)** Increased phosphorylation of ERK1/2 kinase in infant compared to adult T cells. T cells were stimulated by cross-linking with anti-CD3 (10μg) and anti-CD28 (5μg) antibodies for indicated times (or PMA/ionomycin) and examined for pERK1/2 expression by flow cytometry. **(E)** Graphs quantifying fold change (FC) in pERK1/2 expression relative to unstimulated controls for TCR/CD3 crosslinking (left) or PMA/ionomycin (right). Data are compiled from 3 **(A, B, D)** and 2 **(C)** independent experiments. Significance was determined using two-way ANOVA with Sidak multiple comparison testing.

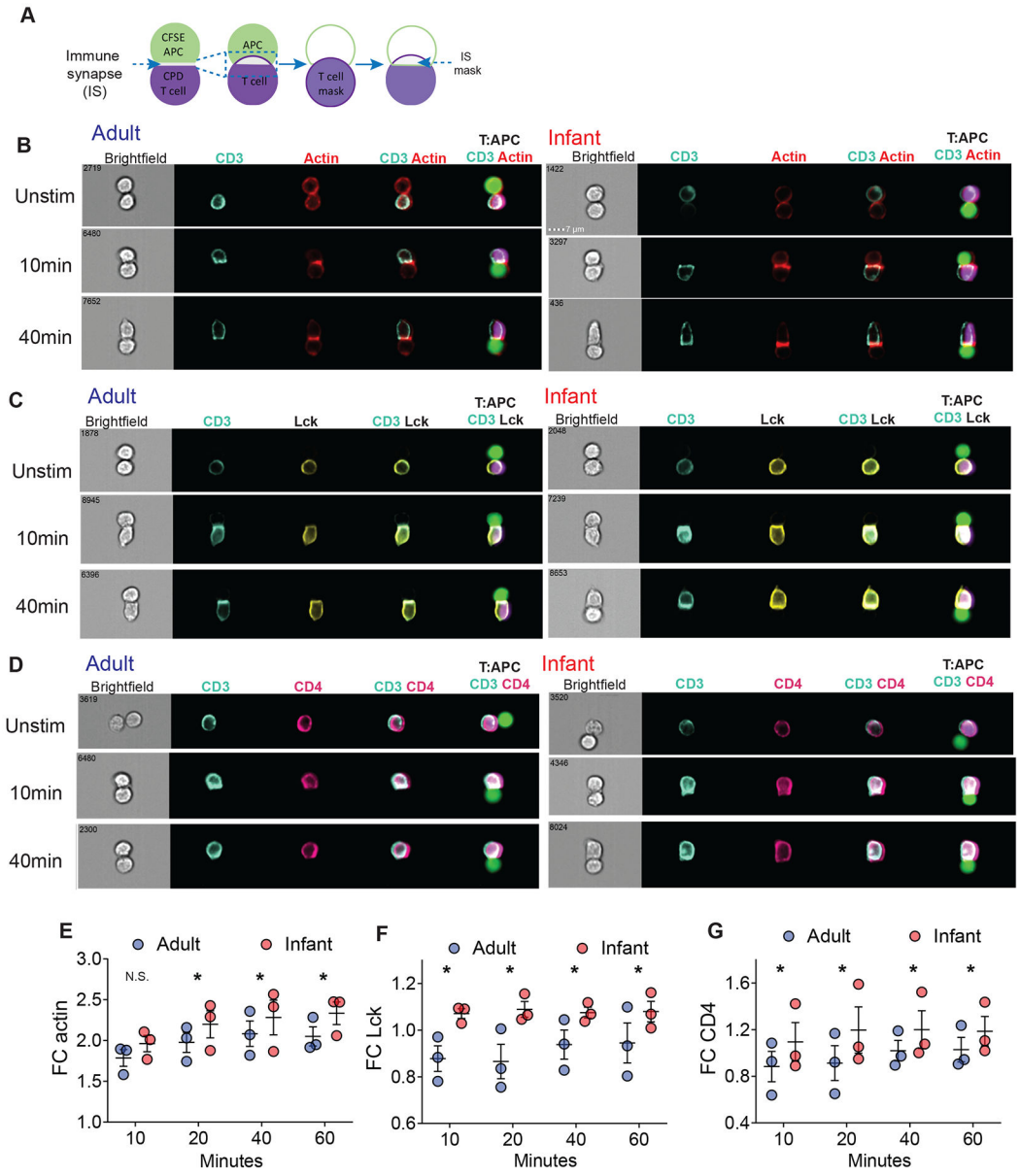

Fig. 6: Infant T cells have higher accumulation of signaling molecules in the immunological synapse compared to adult T cells.

(A) Schematic diagram of ImageStream analysis using IDEAS software to examine accumulation of actin, Lck, and CD4 in the immune synapse of conjugates upon stimulation (see ImageStream Analysis *section* in Materials and Methods). **(B)** Infant T cells compared to adult T cells have higher accumulation of actin (red) with CD3 (turquoise) in T cell:APC conjugates as shown in representative images. OT-II cells were stimulated with 10 μg peptide pulsed APC for indicated times and fixed immediately before staining. **(C)** Infant T cells compared to adult T cells have higher accumulation of Lck (yellow) with CD3 (turquoise) in T cell:APC conjugates as shown in representative images. **(D)** Infant T cells compared to adult T cells have higher accumulation of CD4 (pink) with CD3 (turquoise) in T cell:APC conjugates as shown in representative images. **(E-G)** Graphs quantifying fold

change (FC) of actin **(E)**, Lck **(F)**, and CD4 **(G)** relative to unstimulated control (right). Data are from 3 independent experiments. Significance was determined using two-way ANOVA with Sidak multiple comparison testing.

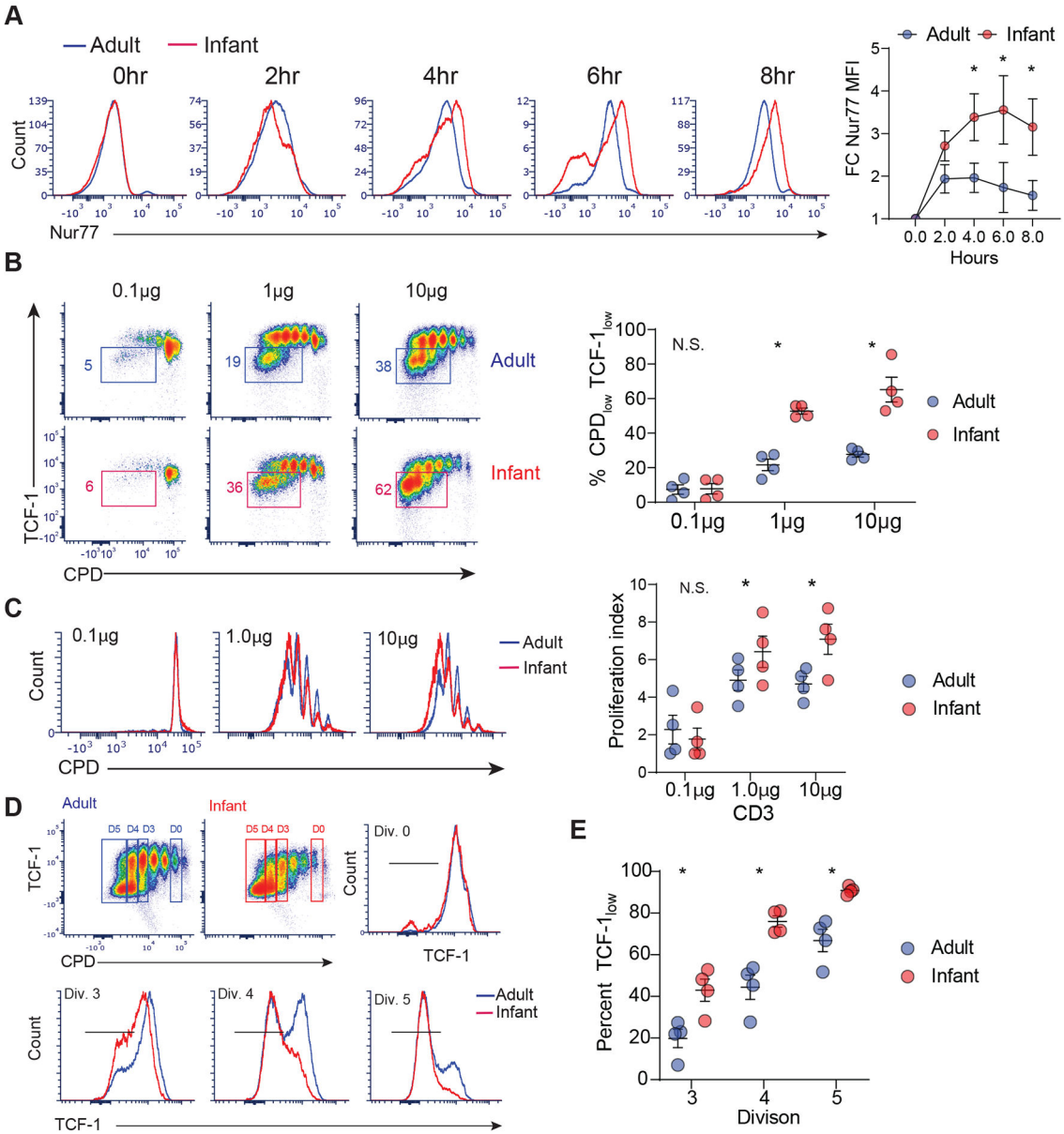

Fig. 7: Human infant T cells exhibit early TCR-coupled signaling and enhanced TCF-1 downregulation.

CD4^{+} naive T cells from human infant and adult lymph nodes were stimulated with anti-CD3/anti-CD28/anti-CD2 coated beads for time points indicated. **(A)** Expression of Nur77 in human infant and adult T cells upon stimulation at the indicated times are shown in representative flow plots (left) and a graph showing Nur77 expression as fold change (FC) relative to unstimulated control (right). **(B)** Expression of TCF-1 as a function of proliferation (CPD expression) after 4 days of stimulation shown in flow cytometry plots (left) and graph with frequencies of infant (red) and adult (blue) T cells that downregulated TCF-1 (right). **(C)** (left) Proliferation of infant (red) and adult (blue) T cells upon varying dose of anti-CD3 stimulation shown in representative flow cytometry plots of proliferation dye dilution (left) and graph showing proliferation index from each independent experiment

(right). **(D)** Expression of TCF-1 by infant and adult T cells following anti-CD3 stimulation (1 μg) as a function CPD dilution in representative flow cytometry dot plots (top row) and histograms of TCF-1 expression by infant (red) and adult (blue) T cells in non-dividing cells (division 0, top row)) and cells undergoing 3-5 divisions (bottom row). **(E)** Graph showing percent TCF_{low} cells (i.e.—TCF-1 downregulated cells) for infant (red) and adult (blue) T cells at indicated divisions for each of three independent experiments. Statistical analysis was done using Student's paired t-test (*$p<0.05$) with error bars representing S.E.M.